Static spherically symmetric Einstein–Vlasov shells made up of particles with a discrete set of values of their angular momentum

2010 Class. Quantum Grav. 27 065008

(http://iopscience.iop.org/0264-9381/27/6/065008)

IOP PUBLISHING CLASSICAL AND QUANTUM GRAVITY

Class. Quantum Grav. **27** (2010) 065008 (17pp) doi:10.1088/0264-9381/27/6/065008

Static spherically symmetric Einstein–Vlasov shells made up of particles with a discrete set of values of their angular momentum

Reinaldo J Gleiser and Marcos A Ramirez

Facultad de Matemática, Astronomía y Física, Universidad Nacional de Córdoba, Ciudad Universitaria, (5000) Córdoba, Argentina

E-mail: gleiser@fis.uncor.edu

Received 7 September 2009, in final form 25 January 2010
Published 22 February 2010
Online at stacks.iop.org/CQG/27/065008

Abstract

In this paper we study static spherically symmetric Einstein–Vlasov shells, made up of equal mass particles, where the angular momentum L of particles takes values only on a discrete finite set. We consider first the case where there is only one value of L, and prove their existence by constructing explicit examples. Shells with either hollow or black hole interiors have finite thickness. Of particular interest is the thin shell limit of these systems, and we study its properties using both numerical and analytic arguments to compare with known results. The general case of a set of values of L is also considered and the particular case where L takes only two values is analyzed, and compared with the corresponding thin shell limit already given in the literature, finding good agreement in all cases.

PACS numbers: 04.50.+h, 04.20.−q, 04.70.−s, 04.30.−w

1. Introduction

Although sometimes sidestepped, it is a general requirement in studying nonvacuum spacetimes in general relativity that the energy momentum tensor, that is, the matter (field) contents, should have a clear, although possibly highly idealized, physical interpretation. Among these choices, the case where matter is described as a large ensemble of particles that interact only through the gravitational field that they themselves, at least partially, create, is of particular interest, both because of their usefulness in modeling physical systems such as star or galaxy clusters, and because of the possibility of a relatively detailed analysis, at least in some restricted cases. As usual in theoretical treatments, one starts imposing as many restrictions as compatible with the central idea, and then tries to generalize from these cases. In this respect, the restriction to static spherically symmetric systems provides an important

simplification, although even with this restriction the problem is far from trivial, and further restrictions have been imposed in order to make significant advances. One of the first concrete examples is that provided by the Einstein model [3], where the particles are restricted to moving on circular orbits. This model is static, and it is not easy to generalize as such to include a dynamical evolution of the system. This generalization can, however, be achieved if the particle world lines are restricted to a shell of vanishing thickness ('thin shell'), as considered by Evans in [2]. The analysis in [2], although motivated by the Einstein model, considers only shells where all the component particles have the same value of their (conserved) angular momentum. In a recent study [1] of the dynamics of spherically symmetric thin shells of counter rotating particles, of which [2] is an example, it was found that the analysis can be extended to shells where the particles have angular momenta that take values on a discrete (but possibly also continuous) set, and are not restricted to single values. It was also found that in the nontrivial thin shell limit of a thick Einstein shell the angular momentum of the particles acquires a unique continuous distribution, and, therefore, the models in [2] and [1] are not approximations to the Einstein model. A relevant question then is what, if any, are the (thick) shells that are approximated by those in [2] and [1]. In this paper we look for an answer to this question by considering a generalization of the Einstein model where instead of circular orbits we impose, at first, the restriction to a single value of the angular momentum. The particle contents are described by a distribution function f in phase space, and, because of the assumption of interaction only through the mean gravitational field, f must satisfy the Einstein–Vlasov equations[1]. In the next section we set up the problem and show that it leads to a well-defined set of equations. In section 3 we set up and analyze a particular model, obtaining expansions for the metric functions at the boundary of the support of f, appropriate for numerical analysis. Further properties are analyzed in section 4, where we show that all these shells have finite mass and thickness. Section 5 contains numerical results for a generic example. The 'thin shell' limit is considered in section 6, both through analytic arguments and a concrete numerical example, with the results showing total agreement with the thin shell results of [1]. A further comparison with [1] is carried out in section 7, where the stability under 'single particle evaporation' of a shell approaching the thin shell limit is considered. The generalization to more than one value of L is given in section 8, where we find that particles with different values of L may be distributed on shells that overlap completely, or do so only partially or not at all. Numerical examples and comparisons with [1] are finally developed in section 9. Some comments and conclusions are given in section 10.

2. The static spherically symmetric Einstein–Vlasov system

The metric for a static spherically symmetric spacetime may be written in the form

$$\mathrm{d}s^2 = -B(r)\,\mathrm{d}t^2 + A(r)\,\mathrm{d}r^2 + h(r)^2\,\mathrm{d}\Omega^2, \tag{1}$$

where $\mathrm{d}\Omega^2 = \mathrm{d}\theta^2 + \sin^2\theta\,\mathrm{d}\phi^2$ is the line element on the unit sphere and $r \geqslant 0$.

For a static, spherically symmetric system, the matter contents, in this case equal mass collisionless particles, are microscopically described by a distribution function $F(r, p^j)$, where $p^j = (p^r, p^\theta, p^\phi)$ are the components of the particle momentum, taken per unit mass. Then, as a consequence of the assumption that the particles move along the geodesics of the spacetime metric, the distribution function F satisfies the Vlasov equation, which, in this case, takes the form

$$p^r \partial_r F - \Gamma^j_{ab} p^a p^b \partial_{p^j} F = 0, \tag{2}$$

[1] For a recent review of the Einstein–Vlasov system and further references see, for example, [6].

where a, b correspond to (t, r, θ, ϕ). It is understood in (2) that p^t is to be computed using $g_{ab}p^a p^b = -1$, so as to satisfy the 'mass shell restriction' $\mu = 1$, where μ is the particles mass. Therefore, in what follows we set

$$p^t = \frac{1}{\sqrt{B(r)}}\sqrt{1 + A(r)(p^r)^2 + h(r)^2[(p^\theta)^2 + \sin^2\theta(p^\phi)^2]}. \tag{3}$$

We also note that $p^t = \mathrm{d}t/\mathrm{d}\tau$, where τ is the proper time along the particle's world line. The Einstein equations for the system are

$$G_{ab} := R_{ab} - \tfrac{1}{2}Rg_{ab} = 8\pi T_{ab}, \tag{4}$$

with the energy momentum tensor given by

$$T_{ab} = -\int F p_a p_b |g|^{1/2}\frac{\mathrm{d}p^r\,\mathrm{d}p^\theta\,\mathrm{d}p^\phi}{p_t}, \tag{5}$$

where g is the determinant of g_{ab}, and $p_a = g_{ab}p^b$. Equations (2), (4) and (5) define the Einstein–Vlasov system restricted to a static spherically symmetric spacetime, with the metric written in the form (1).

The assumption that the metric is static and spherically symmetric implies conservation of the particle's energy:

$$\begin{aligned} E &= B(r)p^t \\ &= \sqrt{B(r)}\sqrt{1 + A(r)(p^r)^2 + h(r)^2[(p^\theta)^2 + \sin^2\theta(p^\phi)^2]} \end{aligned} \tag{6}$$

and of the square of its angular momentum per unit mass,

$$L^2 = h(r)^4[(p^\theta)^2 + \sin^2\theta(p^\phi)^2]. \tag{7}$$

It is easy to check that the Ansatz

$$F(r, p^j) = \Phi(E, L^2), \tag{8}$$

where E and L^2 are functions of r and p^j given by (6), (7) solves the Vlasov equation for an arbitrary function Φ.

To construct and solve explicit models based on (8) for metric (1), it is convenient to change integration variables in (5). We set

$$\begin{aligned} p^\theta &= \frac{1}{h(r)^2}L\cos\chi \\ p^\phi &= \frac{1}{h(r)^2\sin\theta}L\sin\chi \end{aligned} \tag{9}$$

and write (5) in the form

$$T_{ab}(r) = \frac{1}{h(r)^2}\sqrt{\frac{A(r)}{B(r)}}\int \Phi(E, L^2)p_a p_b\frac{L\,\mathrm{d}L\,\mathrm{d}\chi\,\mathrm{d}p^r}{p^t} \tag{10}$$

where we should set

$$\begin{aligned} E &= \sqrt{B\left(1 + (p^r)^2A + \frac{L^2}{h^2}\right)} \\ p^t &= \sqrt{\frac{1}{B}\left(1 + (p^r)^2A + \frac{L^2}{h^2}\right)}. \end{aligned} \tag{11}$$

Andreasson and Rein [7] have explored the properties of models where Φ takes the form

$$\Phi(E, L^2) = \phi(E/E_0)\left(L^2 - L_0^2\right)^\ell. \tag{12}$$

In this paper we consider different types of models, based on the Ansatz

$$\Phi(E, L^2) = F(E)\ \Theta(E_0 - E)\ \delta(L - L_0), \tag{13}$$

where $\Theta(x)$ is the Heaviside step function, and $\delta(x)$ is Dirac's δ; namely, we assume that L takes only the single value L_0, and that there is an upper bound on E, given by E_0. $F(E)$ is assumed to be a smooth function of E. We then have

$$\begin{aligned}
T_t{}^t &= -\frac{4\pi L_0\sqrt{A}}{h^3}\int_0^{p^r_{\max}} F(E)\sqrt{h^2 + L_0^2 + (p^r)^2h^2A}\,\mathrm{d}p^r \\
T_r{}^r &= \frac{4\pi L_0\sqrt{A^3}}{h}\int_0^{p^r_{\max}} \frac{F(E)(p^r)^2}{\sqrt{h^2 + L_0^2 + (p^r)^2h^2A}}\,\mathrm{d}p^r \\
T_\theta{}^\theta &= \frac{2\pi (L_0)^3\sqrt{A}}{h^3}\int_0^{p^r_{\max}} \frac{F(E)}{\sqrt{h^2 + L_0^2 + (p^r)^2h^2A}}\,\mathrm{d}p^r \\
T_\phi{}^\phi &= T_\theta^\theta,
\end{aligned} \tag{14}$$

where $p^r_{\max}$ depends on r and is given by

$$p^r_{\max} = \sqrt{\frac{1}{A(r)}}\sqrt{\frac{E_0^2}{B(r)} - 1 - \frac{L_0^2}{h(r)^2}} \tag{15}$$

if $E_0^2 > B(r)\big(1 + L_0^2/h^2\big)$, and $p^r_{\max} = 0$ otherwise. This simply states the fact that $T_{ab} \neq 0$ only in those regions where a (test) particle with energy E_0 and angular momentum L_0 can actually move.

3. Particular models

We may now use the previous results to construct simple models and analyze their interpretation for a range of possible parameters. This analysis may be carried out in a number of ways. Here we choose the following: we first introduce in (1) a new function $m(r)$ such that $A(r) = (1 - 2m(r)/r)^{-1}$, and change the coordinate r to $\tilde{r} = h(r)$. This amounts to setting

$$\begin{aligned}
h(r) &= r \\
A(r) &= 1/(1 - 2m(r)/r)
\end{aligned} \tag{16}$$

in (1). Then, from the Einstein equations and the form (14) of T_{ab}, we find two independent equations for $m(r)$ and $B(r)$,

$$\begin{aligned}
\frac{\mathrm{d}m}{\mathrm{d}r} &= 4\pi r^2\rho(r) \\
\frac{\mathrm{d}B}{\mathrm{d}r} &= \frac{2B(r)(m(r) + 4\pi r^3 p(r))}{r(r - 2m(r))},
\end{aligned} \tag{17}$$

where $\rho(r) = -T_t{}^t$ is the energy density, and $p(r) = T_r{}^r$ is the radial pressure, given by (14), with $h(r) = r$. There is also an equation for $p_T(r) = T_\theta{}^\theta$, but, as can be checked, this is not independent of (17). Equations (17) are deceptively simple, because the explicit dependence of ρ and p on m and B is in general quite complicated. Here we consider a simple example and propose a method for constructing the solutions, which is illustrated by the example. We recall that the main purpose of our analysis is to find examples of thick shells that have the

thin shell limit used in [1]. A sufficiently simple yet nontrivial example is obtained with the choice

$$F(E) = Q_1 E = Q1\sqrt{B\left(1 + (p^r)^2 A + \frac{L^2}{r^2}\right)}, \tag{18}$$

where $Q_1 \geqslant 0$ is a constant. With this choice we may perform the integrals in (14) explicitly and, after some simplifications, we obtain

$$\frac{\mathrm{d}m}{\mathrm{d}r} = \frac{Q_2\left[2\left(L_0^2 + r^2\right)B + r^2E_0^2\right]\sqrt{r^2E_0^2 - \left(L_0^2 + r^2\right)B}}{r^3 B} \tag{19}$$

$$\frac{\mathrm{d}B}{\mathrm{d}r} = \frac{2mB}{r(r-2m)} + \frac{2Q_2\left[r^2E_0^2 - \left(L_0^2 + r^2\right)B\right]^{3/2}}{r^3(r-2m)}, \tag{20}$$

where $Q_2 = 16\pi^2 L_0 Q_1/3$. We also find

$$\begin{aligned}
\rho(r) &= \frac{Q_2\left[2\left(L_0^2 + r^2\right)B + r^2E_0^2\right]\sqrt{r^2E_0^2 - \left(L_0^2 + r^2\right)B}}{4\pi r^5 B} \\
p(r) &= \frac{Q_2\left[r^2E_0^2 - \left(L_0^2 + r^2\right)B\right]^{3/2}}{4\pi B r^5} \\
p_T(r) &= \frac{3Q_2L_0^2\sqrt{r^2E_0^2 - \left(L_0^2 + r^2\right)B}}{8\pi r^5}.
\end{aligned} \tag{21}$$

Considering (19), (20), we find that it is a simple, but rather difficult to handle, system of equations for $m(r)$ and $B(r)$. We have not found closed (analytical) solutions for the system, and, therefore, we must resort to numerical methods. The application of these methods requires, however, considering and solving several subtleties inherent in the system. As indicated above, in all these equations ((19), (20) and (21)), the terms involving Q_2 should be set equal to zero if $r^2E_0^2 \leqslant \left(L_0^2 + r^2\right)B$. We note that for $Q_1 = Q_2 = 0$ we have $m(r) = M$, with $M =$ constant, and $B(r) = (1 - 2M/r)C_0$, where C_0 is also a constant, corresponding to the standard Schwarzschild solution. For a shell-type solution, these solutions correspond to the inner and outer regions, to be matched to the region where $T_{ab} \neq 0$. When $Q_1 \neq 0$, since we must have $B(r) > 0$, we must also have $\mathrm{d}m/\mathrm{d}r \geqslant 0$, but, even though $\rho \geqslant 0$ we might end up with $m(r) < 0$, and still have all equations satisfied. This would be the case, for instance, if in the inner region we have a Schwarzschild spacetime with negative mass (naked singularity).

For shell like solutions, either with an empty interior or with a central mass (black hole), a further difficulty can be seen considering that there should exist an 'allowed region' where $r^2E_0^2 \geqslant \left(L_0^2 + r^2\right)B$, with r taking values in the interval $r_i \leqslant r \leqslant r_o$, where r_i and r_o are, respectively, the inner and outer radii of the shell. We must impose continuity in both $B(r)$ and $m(r)$ to avoid δ functions in T_{ab}. This implies that $r^2E_0^2 - \left(L_0^2 + r^2\right)B$ is continuous in $r_i \leqslant r \leqslant r_o$ and approaches continuously the value zero at the boundaries. Therefore, both $\mathrm{d}m/\mathrm{d}r$ and $\mathrm{d}B/\mathrm{d}r$ are also continuous inside and at the boundaries of this interval, and actually we have $\mathrm{d}m/\mathrm{d}r|_{r=r_i} = 0$. We also find that $\mathrm{d}^2B/\mathrm{d}r^2$ should be continuous, but $\mathrm{d}^2m/\mathrm{d}r^2$ must be singular, and this makes the construction of numerical solutions where we try to fix from the beginning the values of r_i and r_o rather difficult. Nevertheless, the above analysis indicates that for $r > r_i$, but $r \sim r_i$, we should have

$$\begin{aligned}
B(r) &= B_0 + B_1(r - r_i) + B_2(r - r_i)^2 + \mathcal{R}_B \\
m(r) &= M_1 + \mathcal{R}_m,
\end{aligned} \tag{22}$$

where B_0, B_1 and M_1 are constants and $\mathcal{R}_B$ and $\mathcal{R}_m$ are functions of r that vanish respectively faster than $(r-r_i)^2$ and $(r-r_i)$ for $r-r_i \to 0^+$. It is straightforward to extend this analysis to a higher order by imposing consistency between the right- and left-hand sides of (19), (20) as $r-r_i \to 0^+$. We find

$$\begin{aligned} B(r) &= B_0 + B_1(r-r_i) + B_2(r-r_i)^2 + B_3(r-r_i)^{5/2} + \tilde{\mathcal{R}}_B \\ m(r) &= M_1 + M_2(r-r_i)^{3/2} + M_3(r-r_i)^{5/2} + \tilde{\mathcal{R}}_m, \end{aligned} \tag{23}$$

where B_2, B_3, M_2 and M_3 are constants, and $\tilde{\mathcal{R}}_B$ and $\tilde{\mathcal{R}}_m$ stand for higher order terms. The constants appearing in (23) are not independent. They may be written, e.g., in terms of r_i, M_1, L_0, E_0 and Q_2. We note that M_1 is the Schwarzschild mass for the region inside the shell ($r \leqslant r_i$). Moreover, the system (19), (20) is invariant under the the rescaling $B \to \lambda B$, $E_0 \to \sqrt{\lambda}E_0$ and $Q_2 \to Q_2/\sqrt{\lambda}$. It will prove convenient to use this scaling invariance, and the continuity of $B(r)$ to set

$$B(r_i) = 1 - \frac{2M_1}{r_i} \tag{24}$$

so that the solution for $r < r_i$ takes the standard Schwarzschild form. On the other hand, the condition that $r = r_i$ corresponds to the inner boundary of the shell implies

$$B_0 = \frac{r_i^2 E_0^2}{r_i^2 + L_0^2} \tag{25}$$

and, therefore, we set

$$\begin{aligned} B_0 &= 1 - \frac{2M_1}{r_i} \\ E_0^2 &= \frac{\left(L_0^2 + r_i^2\right)(r_i - 2M_1)}{r_i^3}. \end{aligned} \tag{26}$$

Similarly, we find

$$\begin{aligned} B_1 &= \frac{2M_1}{r_i^2} \\ B_2 &= -\frac{2M_1}{r_i^3} \\ B_3 &= \frac{8\sqrt{2}Q_2\left[(2r_i - 3M_1)L_0^2 + (r_i - M_1)r_i^2\right]\sqrt{(r_i - 3M_1)L_0^2 - M_1 r_i^2}}{5(r_i - 2M_1)r_i^6} \\ M_2 &= \frac{2\sqrt{2}Q_2\left(L_0^2 + r_i^2\right)\sqrt{(r_i - 3M_1)L_0^2 - M_1 r_i^2}}{r_i^4}. \end{aligned} \tag{27}$$

The explicit expression for M_3, as well as for higher order coefficients, is also easily obtained but is rather long and will not be included here, although it was used in the numerical computations described below.

The philosophy that we adopt here is to assume that the inner radius r_i and inner mass M_1 are given. Then, in accordance with (27), a nontrivial solution exists only if $r_i > 3M_1$. Next, we assume that L_0 is also given. Again, from (27), it must satisfy

$$L_0^2 > \frac{M_1 r_i^2}{r_i - 3M_1}. \tag{28}$$

Accordingly, given some fixed values of r_i, M_1 and L_0 satisfying the above conditions, we may construct families of solutions depending on the single parameter Q_2 by solving the nontrivial part of equations (19) and (20), with E_0 given by (26). In the next section we explore some properties of the resulting models.

4. Some general properties

An interesting question regarding the model of the previous section is related to the possible values that the mass and thickness of the shells can attain. For the Ansatz (12) this problem was analyzed in a series of papers by Rein, Rendall and Andreasson (see e.g. [4, 5], and also [6] for a review and more extensive references). The general result is that under some further (mild) restrictions on the form (12) such shells exist and have finite thickness and finite mass. The rigorous proofs obtained by these authors are somewhat dependent on the form assumed for the distribution function. In particular, the dependence on L assumed by those authors does not appear to have a simple distributional limit of the form assumed here. Nevertheless, the proofs can probably be extended to more general assumptions regarding this function, for instance, to include our particular models with a distributional dependence on the angular momentum. On this account, since we were interested in constructing particular examples, rather than analyzing the more general case, we found it simpler to obtain their general properties directly by studying the solutions of the system (19), (20), assuming that initial data of the form described in the previous section are given. As shown below, although the models constructed with our prescription may differ considerably in detail from those obtained using (12), they also correspond to shells with finite mass and thickness, whose interior can be empty space, a black hole or even a negative mass naked singularity.

As a starting point, we may show that $m(r)$ must be bounded by $r/2$ as follows. First, from (19), (20) we have that $\mathrm{d}B/\mathrm{d}r > 0$, $\mathrm{d}m/\mathrm{d}r \geqslant 0$, and, therefore, both $m(r)$ and $B(r)$ are increasing functions of r. But also from these equations we have the bounds

$$r_i^2 E_0^2 \big/ \big(L_0^2 + r_i^2\big) \leqslant B(r) \leqslant r^2 E_0^2 \big/ \big(L_0^2 + r^2\big), \tag{29}$$

where r_i is the inner radius of the shell. This implies that $\mathrm{d}m/\mathrm{d}r$ is finite, and, therefore, near a point $r = r_s$, where $m(r)$ approaches $r_s/2$, we should have

$$m(r) = \tfrac{1}{2} r_s + m_1 (r - r_s) + \cdots, \tag{30}$$

where $m_1 > 0$ is finite and the dots indicate terms that vanish faster than $r - r_s$ as $r \to r_s$. Replacing in (20) we find that $\mathrm{d}B/\mathrm{d}r$ would diverge as $(r - r_s)^{-1}$, and therefore, $B(r)$ would diverge as $\ln(r_s - r)$, which is incompatible with the bounds (29) satisfied by $B(r)$, and, therefore, all the solutions must satisfy $m(r) < r/2$.

Similarly, we find that the shells must have finite thickness by considering the limit of the solutions of the system (19), (20) as $r \to \infty$, under the restriction that $\rho \neq 0$, and the condition just proved that $r > 2m(r)$. The first, according to (19), (20) and (21), implies $B(r) < E_0^2$, and then, if the shell extends to $r = \infty$, we should have $B_\infty = \lim_{r\to\infty} B(r) \leqslant E_0^2$. We remark that $\mathrm{d}B/\mathrm{d}r \geqslant 0$. Therefore, $B(r)$ must approach a finite value B_∞ monotonically from below. Consider first the case $B_\infty < E_0^2$. Replacing in the first equation in (19), (20), for large r we find that $\mathrm{d}m/\mathrm{d}r$ approaches a constant value, and, therefore, $m(r)$ grows linearly with r. But then, replacing in the second equation in (19), (20), we find that $\mathrm{d}B/\mathrm{d}r$ decreases as $1/r$, leading to a logarithmic growth in $B(r)$, incompatible with the assumed conditions. Therefore, any possible solution that extends to $r = \infty$ should have $B_\infty = E_0^2$. Then, for large r we should have

$$B(r) = \frac{E_0^2 r^2}{L_0^2 + r^2} - B_1(r) \tag{31}$$

with $B_1(r) \to 0$, as $r \to \infty$. Replacing now in (19), (20), to the leading order we find

$$\frac{\mathrm{d}m}{\mathrm{d}r} \simeq 3 Q_2 \sqrt{B_1} \tag{32}$$

and this implies that $m(r)/r \to 0$ as $r \to \infty$. Then, using again (19), (20), we should have

$$\frac{\mathrm{d}B_1}{\mathrm{d}r} \simeq -\frac{2E_0^3 Q_2}{r} \tag{33}$$

and this implies that $B_1(r) \simeq -2E_0^3 Q_2 \ln(r)$, which contradicts the assumption $B_1(r) \to 0$. Thus, we conclude that the solution cannot be extended to $r = \infty$, and, therefore, the equation

$$E_0^2 r^2 - \left(L_0^2 + r^2\right) B(r) = 0 \tag{34}$$

must always be satisfied for some $r = r_o$, where r_o is finite and corresponds to the outer radius of the shell, which, in turn, implies that the total mass $M_2 = m(r_o)$ is bounded by the condition $M_2 < r_o/2$. This result is in agreement with the general bounds found in [9] in the case of an empty interior.

We thus conclude that *all shells constructed in accordance with prescription* (18) *have finite mass and finite thickness*.

We nevertheless believe that this result is more general, and applies to all shells satisfying Ansatz (13), although we do not have a complete proof of this statement.

5. Numerical results

As indicated, we do not have closed solutions of the equations for $B(r)$ and $m(r)$, even for the simple model of the previous sections. Nevertheless, since (19), (20) is a first-order ODE system, we can apply numerical methods to analyze it. We may use the expansions (23), disregarding the terms in $\tilde{\mathcal{R}}_B$ and $\tilde{\mathcal{R}}_m$, to obtain appropriate initial values for $B(r)$ and $m(r)$, for r close to r_i, in the nontrivial region $r > r_i$.

We may illustrate this point with a particular example. We take $r_i = 7.0$, $M_1 = 1.0$, $L_0 = 4$, $E_0 = 1$ and $Q_2 = 0.1$. Using these values and (23) (truncated as indicated above), we find $B(7.0001) = 0.7538\ldots$, and $m(7.0001) = 1.0000\ldots$ (actually, the computations were carried out to 30 digits, using a Runge–Kutta integrator). The numerical results are plotted in figures 1 and 2.

6. Thin shells

One of the motivations for studying the type of shells considered in this paper is the possible existence of a nontrivial 'thin shell' limit, where the thickness of the shell goes to zero, with the restriction to a single or a finite set of values of L, and how this limit compares with the thin shells considered in [2] and [1]. We remark that the existence of thin shell limits of Einstein–Vlasov systems has already been analyzed in the literature [8], but with a different purpose in mind. Here we are interested not only in the existence of this limit for our particular models, but especially in the limiting values of the parameters characterizing our shells. Since this type of analysis is not immediately included in, e.g, [8], we consider it relevant to provide an explicit proof of the properties of our models in the thin shell limit. The construction will proceed in two steps. First we assume some fixed values of r_i, M_1 and L_0 are given. In accordance with the arguments of section 4, for every choice of Q_2 the shell has an outer boundary at some finite $r_o > r_i$. If we look now at (19), (20), it is clear that for large Q_2, the behavior of both $\mathrm{d}B/\mathrm{d}r$ and $\mathrm{d}m/\mathrm{d}r$ is governed by that of the expression $\xi(r) = E_0^2 r^2 - \left(L_0^2 + r^2\right) B(r)$, which

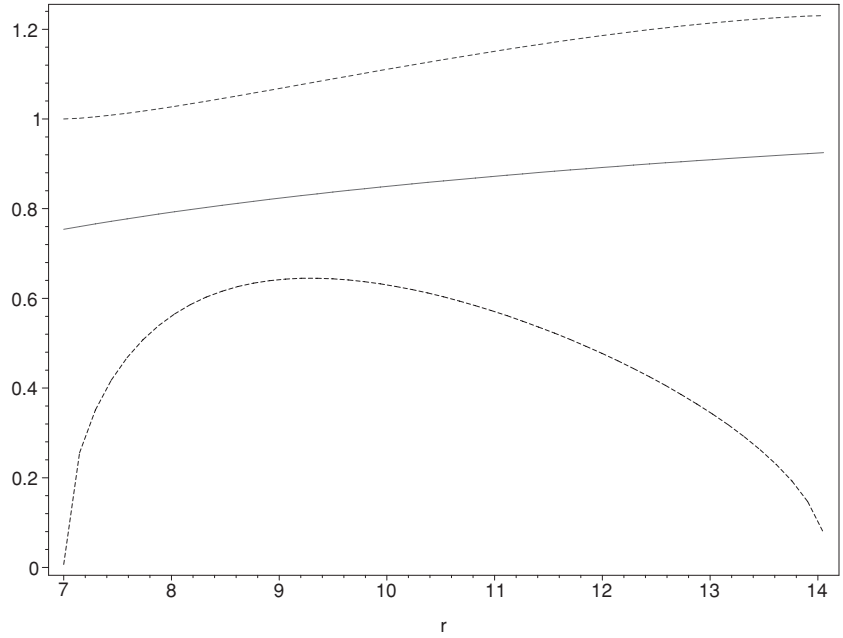

Figure 1. Plots of $m(r)$ (dotted, upper curve), $B(r)$ (solid, middle curve) and $15(\mathrm{d}m/\mathrm{d}r)$ (dashed, lower curve), as functions of r for $r_i = 7.0$, $M_1 = 1.0$, $L_0 = 4$, $E_0 = 1$ and $Q_2 = 0.1$. The end point of the plot is at $r_o = 14.1098\ldots$, with $B(r_o) = 0.9256\ldots$ and $M_2 = m(r_o) = 1.2306\ldots$

must satisfy $\xi > 0$ within the shell. For $r > r_i$, but sufficiently near r_i, we have

$$\xi(r) \simeq \frac{2(r_i - 3M_1)L_0^2 - M_1 r_i^2}{r_i^2}(r - r_i) \tag{35}$$

and, therefore, $\xi(r)$ is an increasing function close to r_i. We note, however, that for $\xi \neq 0$, equation (20) implies that $\mathrm{d}B/\mathrm{d}r$ can be made arbitrarily large by taking Q_2 appropriately large. This implies that $B(r)$ itself will also be increasing arbitrarily fast, and therefore we should have that $\xi(r)$ starts decreasing and approaches zero at an arbitrarily close distance from r_i. Here we have two possibilities. The first is that $\xi(r)$ effectively becomes zero at some $r = r_\xi$, with $r_\xi \to r_i^+$ as $Q_2 \to \infty$, and therefore the thickness of the shell becomes arbitrarily thin as $Q_2 \to \infty$. The second is that, in contrast, $\xi(r)$ remains nonvanishing, but sufficiently small so that $\mathrm{d}m/\mathrm{d}r$ (controlled by $Q_2\sqrt{\xi}$), remains small, but nonvanishing. This implies that we should have

$$B(r) = \frac{E_0^2 r^2}{L_0^2 + r^2} - \chi(r)^2, \tag{36}$$

where $\chi(r) = \sqrt{\xi(r)}$ is small and decreases as Q_2 increases. Now, we may solve (20) for $m(r)$, and replacing in (19) we obtain a second-order equation that contains only $B(r)$, and its first- and second-order derivatives. Replacing (36) in this equation, and expanding to the lowest order in $1/Q_2$, we obtain

$$\chi(r) = \frac{\left(3L_0^2 - r^2\right)r^3 L_0^2}{3Q_2\left(L_0^2 + r^2\right)\left(3L_0^2 + r^2\right)} + \mathcal{O}\left(Q_2^{-2}\right). \tag{37}$$

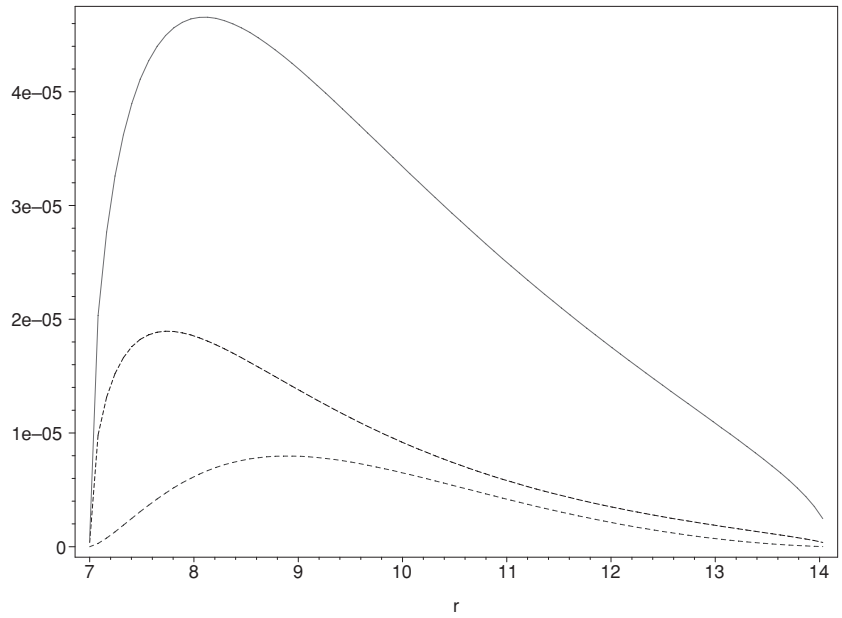

Figure 2. Plots of $\rho(r)$ (solid, upper curve), $4p_T(r)$ (dashed, middle curve) and $40p(r)$ (dotted, lower curve), as functions of r for $r_i = 7.0$, $M_1 = 1.0$, $L_0 = 4$, $E_0 = 1$ and $Q_2 = 0.1$. The end point of the plot is at $r_o = 14.1098\ldots$, with $B(r_o) = 0.9256\ldots$ and $M_2 = m(r_o) = 1.2306\ldots$

Next we replace both (36) and (37) in (19), and in (20) solved for $m(r)$. From these two equations we find, respectively,

$$\frac{\mathrm{d}m}{\mathrm{d}r} = \frac{\left(3L_0^2 - r^2\right)L_0^2}{\left(3L_0^2 + r^2\right)^2} + \frac{1}{Q_2^2}\phi_1(r) + +\mathcal{O}\left(Q_2^{-3}\right), \tag{38}$$

where $\phi_1(r)$ is a finite function of r, and

$$\frac{\mathrm{d}m}{\mathrm{d}r} = \frac{\left(3L_0^2 - r^2\right)L_0^2}{\left(3L_0^2 + r^2\right)^2} + \frac{1}{Q_2^2}\phi_2(r) + \mathcal{O}\left(Q_2^{-3}\right), \tag{39}$$

where $\phi_2(r)$ is also a finite function of r, but with $\phi_1(r) \neq \phi_2(r)$. We must therefore conclude that the behavior given by (36) is incompatible with the system (19, 20), and the thickness of the shell must go to zero as $Q_2 \to \infty$. We remark that this behavior is clearly seen in the numerical computations we have carried out. The foregoing result is qualitative, in the sense that we do not obtain a quantitative relation between the parameters and the shell thickness given, e.g., by $r_o - r_i$, but it proves that $r_o \to r_i$ as $Q_2 \to \infty$. This result is, nevertheless, all that we need to find the relevant shell parameters in the limit $Q_2 \to \infty$.

We first recall that for a static thin shell constructed according to Evans' prescriptions [2], we have the following relation between the radius R, inner (M_1) and outer (M_2) mass, and angular momentum $\tilde{L}_0$ of the particles,

$$\tilde{L}_0^2 = \frac{R - \sqrt{R - 2M_1}\sqrt{R - 2M_2}}{3\sqrt{R - 2M_1}\sqrt{R - 2M_2} - R}. \tag{40}$$

We may now prove that the nontrivial thin shell limits of the shells constructed according to prescription (18) effectively coincide with the Evans shells of [2] as follows. We first take

the r derivative of (20), and then use (19) and (20), to obtain

$$\frac{\mathrm{d}^2B}{\mathrm{d}r^2} = \frac{\left[r(2E^2r^2+(r^2+L^2)B)\frac{\mathrm{d}B}{\mathrm{d}r}+2(4E^2r^2+(2L^2-r^2)B)\right]}{r(E^2r^2+2(L^2+r^2)B)(r-2m)}\frac{\mathrm{d}m}{\mathrm{d}r} - \frac{4}{r^2(r-2m)}\left[r(r-2m)\frac{\mathrm{d}B}{\mathrm{d}r}-mB\right]. \tag{41}$$

Next let r_i and r_o be, respectively, the inner and outer radii of the shell, and $M_1 = m(r_i)$ and $M_2 = m(r_o)$ the corresponding masses inside and outside the shell. Then, for $r_i \leqslant r \leqslant r_o$ we have $\mathrm{d}B/\mathrm{d}r > 0$, and

$$\left.\frac{\mathrm{d}B}{\mathrm{d}r}\right|_{r=r_i} = \frac{2M_1B(r_i)}{r_i(r_i-2M_1)}; \qquad \left.\frac{\mathrm{d}B}{\mathrm{d}r}\right|_{r=r_o} = \frac{2M_2B(r_o)}{r_o(r_o-2M_2)}. \tag{42}$$

The idea now is to use the fact that

$$\begin{aligned} &\int_{r_i}^{r_o}\frac{\mathrm{d}^2B}{\mathrm{d}r^2}\,\mathrm{d}r = \left.\frac{\mathrm{d}B}{\mathrm{d}r}\right|_{r=r_o} - \left.\frac{\mathrm{d}B}{\mathrm{d}r}\right|_{r=r_i} = \frac{2M_2B(r_o)}{r_o(r_o-2M_2)} - \frac{2M_1B(r_i)}{r_i(r_i-2M_1)};\\ &\int_{r_i}^{r_o}\frac{\mathrm{d}m}{\mathrm{d}r}\,\mathrm{d}r = M_2 - M_1. \end{aligned} \tag{43}$$

On this account we rewrite (41) in the form

$$\frac{1}{r-2m}\frac{\mathrm{d}m}{\mathrm{d}r} = \frac{r(E^2r^2+2B(L^2+r^2))}{\left[r(2E^2+(r^2+L^2)B)\frac{\mathrm{d}B}{\mathrm{d}r}+2(4E^2r^2+(2L^2-r^2)B)\right]}\frac{\mathrm{d}^2B}{\mathrm{d}r^2} + \frac{4(E^2r^2+2B(L^2+r^2))\left[r(r-2m)\frac{\mathrm{d}B}{\mathrm{d}r}-mB\right]}{r(r-2m)\left[r(2E^2+(r^2+L^2)B)\frac{\mathrm{d}B}{\mathrm{d}r}+2(4E^2r^2+(2L^2-r^2)B)\right]} \tag{44}$$

and integrate both sides from $r = r_i$ to $r = r_o$. But now we notice that while both $m(r)$ and $\mathrm{d}B/\mathrm{d}r$ are rapidly changing but bounded in $r_i \leqslant r \leqslant r_o$, the change of $B(r)$, and r in that interval is only of order $r_o - r_i$. We may then choose a point $r = R$, with $r_i < R < r_o$, and set $B(r) = B(R) = B_0$, and $r = R$, except in the arguments of $m(r)$, $\mathrm{d}m/\mathrm{d}r$, $\mathrm{d}B(r)/\mathrm{d}r$ and $\mathrm{d}^2B(r)/\mathrm{d}r^2$, in (44), as this introduces errors at most of order $r_o - r_i$, in the factors of $\mathrm{d}m/\mathrm{d}r$, and $\mathrm{d}^2B(r)/\mathrm{d}r^2$, and in the last term on the right-hand side of (44). Similarly, we may set $E^2 = (L^2+R^2)B_o/R^2$ in (44), to obtain, up to terms of order $r_o - r_i$,

$$\frac{1}{R-2m(r)}\frac{\mathrm{d}m}{\mathrm{d}r} = \frac{R(L^2+R^2))}{R(R^2+L^2))\frac{\mathrm{d}B}{\mathrm{d}r}+2(R^2+2L^2)B_0}\frac{\mathrm{d}^2B}{\mathrm{d}r^2} + \frac{4((L^2+R^2))\left[R(R-2m)\frac{\mathrm{d}B}{\mathrm{d}r}-mB_0\right]}{R(R-2m)\left[R(R^2+L^2)\frac{\mathrm{d}B}{\mathrm{d}r}+2(R^2+2L^2)B_0\right]} \tag{45}$$

and, again, we note that the last term on the right-hand side of (45) gives a contribution of order $r_o - r_i$. We then conclude that

$$\lim_{r_o\to r_i}\int_{r_i}^{r_o}\frac{1}{R-2m(r)}\frac{\mathrm{d}m}{\mathrm{d}r}\mathrm{d}r = \lim_{r_o\to r_i}\int_{r_i}^{r_o}\frac{R(L^2+R^2))}{R(R^2+L^2))\frac{\mathrm{d}B}{\mathrm{d}r}+2(R^2+2L^2)B_0}\frac{\mathrm{d}^2B}{\mathrm{d}r^2}\,\mathrm{d}r. \tag{46}$$

The integration of the terms in $\mathrm{d}m/\mathrm{d}r$, and $\mathrm{d}^2B(r)/\mathrm{d}r^2$, is now straightforward. We use next (42) and the fact that in this limit $B(r_i) = B_0 = B(r_o)$ and $r_i = R = r_o$, to obtain

$$\frac{\sqrt{R-2M_1}}{\sqrt{R-2M_2}} = \frac{(R-2M_1)(R^3+2RL^2-3M_2L^2-M_2R^2)}{(R-2M_2)(R^3+2RL^2-3M_1L^2-M_1R^2)}. \tag{47}$$

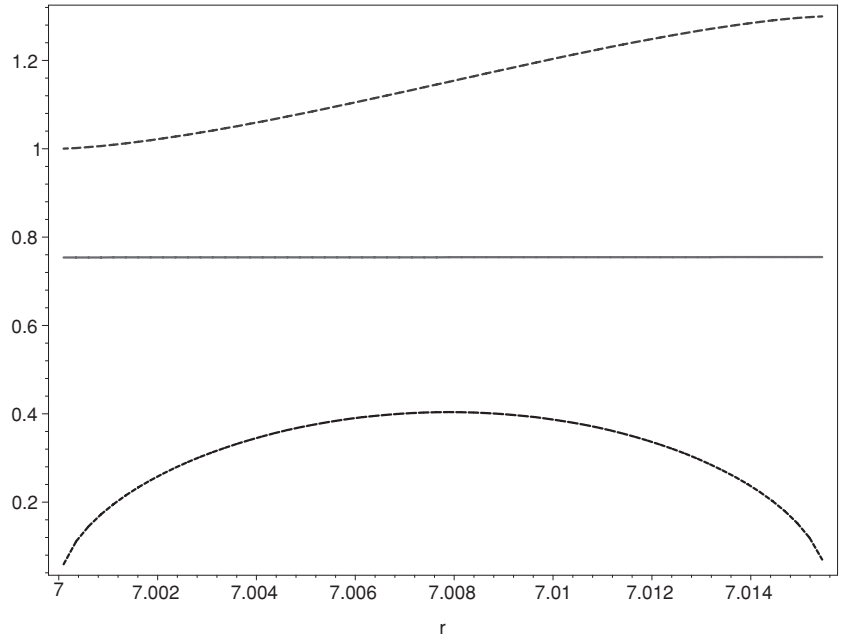

Figure 3. Plots of $m(r)$ (dotted, upper curve), $B(r)$ (solid, middle curve) and 10ρ (dashed, lower curve), as functions of r for $r_i = 7.0$, $M_1 = 1.0$, $L_0 = 4$, $E_0 = 1$ and $Q_2 = 800$. The end point of the plot is at $r_o = 7.0155\ldots$, with $B(r_o) = 0.7546\ldots$ and $M_2 = m(r_o) = 1.2999\ldots$

Solving this equation for L^2, we finally find

$$L^2 = \frac{R^2(R - \sqrt{R-2M_1}\sqrt{R-2M_2})}{3\sqrt{R-2M_1}\sqrt{R-2M_2} - R}, \tag{48}$$

which is, precisely, the relation satisfied by the parameters of the shells of (40).

We can also check this result, and, in turn, the accuracy of numerical codes, by directly considering initial data for the numerical integration that effectively lead to shells where the thickness is a small fraction of the radius.

A particular example is given in figure 3, where the values of the initial data are also indicated. We can see that the mass increases by about 30%, while the thickness of the shell is less than 0.3% of the shell radius. We can check that these results are in agreement with (40). Solving this for M_2,

$$M_2 = \frac{R\left[2(R-3M_1)R^2\tilde{L}_0^2 + (4R-9M_1)\tilde{L}_0^4 - M_1R^4\right]}{(R-2M_1)\left(R^2+3\tilde{L}_0^2\right)^2}, \tag{49}$$

and replacing $\tilde{L}_0 = 4$, $M_1 = 1$ and $R = 7$, we find $M_2 = 1.2997\ldots$ in very good agreement with the numerical results quoted in figure 3.

7. Stability under 'single particle evaporation'

A complete analysis of the stability of the shells is out of the scope of the present research. Nevertheless, we may rather easily analyze their stability under 'single particle evaporation'. This refers to the possibility that a particle approaching the boundary of the shell becomes

eventually unbounded and leaves the shell. Some examples of this behavior for thin shells were analyzed in [1]. In our case we consider a shell approaching the thin shell limit. We restrict to the case of vanishing inner mass $M_1 = 0$. If r_i and r_o are, respectively the inner and outer boundaries of the shell, the matching conditions in the absence of singular shells at r_i and r_o imply that both $m(r)$ and $B(r)$ and their first derivatives should be continuous at both $r = r_i$ and $r = r_o$. The form (1) of the metric with choice (16) implies that for $0 \leqslant r \leqslant r_i$ we have

$$\mathrm{d}s^2 = -B_i\,\mathrm{d}t^2 + \mathrm{d}r^2 + r^2\,\mathrm{d}\Omega^2, \tag{50}$$

where $B_i > 0$ is a constant. Then, at $r = r_i$ we have

$$B_i = \frac{r_i^2 E_0^2}{L_0^2 + r_i^2}. \tag{51}$$

For $r \geqslant r_o$, the metric takes the form

$$\mathrm{d}s^2 = -\frac{(r - 2M_2)r_o}{(r_o - 2M_2)r} B_o\,\mathrm{d}t^2 + \frac{r}{r - 2M_2}\,\mathrm{d}r^2 + r^2\,\mathrm{d}\Omega^2, \tag{52}$$

where $B_o > 0$ is another constant satisfying

$$B_o = \frac{r_o^2 E_0^2}{L_0^2 + r_o^2}. \tag{53}$$

Consider now a test particle moving along a geodesic of the shell spacetime, with 4-velocity $U^\mu(\tau) = (\mathrm{d}t/\mathrm{d}\tau, \mathrm{d}r/\mathrm{d}\tau, \mathrm{d}t\theta/\mathrm{d}\tau, \mathrm{d}\phi/\mathrm{d}\tau)$, with $U^\mu U_\mu = -1$. Without loss of generality we may choose $\mathrm{d}\theta/\mathrm{d}\tau = 0$. Then we have the constants of the motion:

$$E = B(r)\frac{\mathrm{d}t}{\mathrm{d}\tau}, \quad L = r^2\frac{\mathrm{d}\phi}{\mathrm{d}\tau} \tag{54}$$

and the normalization of U^μ implies

$$\left(\frac{\mathrm{d}r}{\mathrm{d}\tau}\right)^2 = \frac{E^2}{B(r)}\left(1 - \frac{2m(r)}{r}\right) - \left(1 + \frac{L^2}{r^2}\right)\left(1 - \frac{2m(r)}{r}\right). \tag{55}$$

Therefore, for $r \geqslant r_o$ we have

$$\left(\frac{\mathrm{d}r}{\mathrm{d}\tau}\right)^2 = \frac{E^2}{B_o}\left(1 - \frac{2M_2}{r_o}\right) - \left(1 + \frac{L^2}{r^2}\right)\left(1 - \frac{2M_2}{r}\right) \tag{56}$$

and the particle radial acceleration is given by

$$\frac{\mathrm{d}^2 r}{\mathrm{d}\tau^2} = \frac{L^2}{r^3} - \frac{(3L^2 + r^2)M_2}{r^4}. \tag{57}$$

If we assume now that the shell is close to the thin shell limit, with angular momentum L_0, radius R (with $r_i < R < r_o$) and mass M_2, then we should have

$$L_0^2 = \frac{(\sqrt{R} - \sqrt{R - 2M_2})R^2}{3\sqrt{R - 2M_2} - \sqrt{R}}. \tag{58}$$

Then, for $L \simeq L_0$, and $r \simeq R \simeq r_o$ we find

$$\frac{\mathrm{d}^2 r}{\mathrm{d}\tau^2} \sim -\frac{2\sqrt{R - 2M_2}(\sqrt{R} - \sqrt{R - 2M_2})}{R^{3/2}(3\sqrt{R - 2M_2} - \sqrt{R})} < 0. \tag{59}$$

Similarly, in the region $0 \leqslant r \leqslant r_i$, for $r \sim r_i \sim R$ we find

$$\frac{\mathrm{d}^2 r}{\mathrm{d}\tau^2} \sim \frac{2(\sqrt{R} - \sqrt{R - 2M_2})}{R(3\sqrt{R - 2M_2} - \sqrt{R})} > 0 \tag{60}$$

and, therefore, all these shells are stable under 'single particle evaporation', in total agreement with the results of [1].

A different problem is that of the dynamical stability of the shell as a whole. A numerical investigation of this problem is given in [10]. A different approach, applicable only to 'thin' shells, was also analyzed in [1]. In this case the motion is described by ordinary differential equations for the shell radius R as a function, e.g., of proper time on the shell, which allows for a significant simplification of the treatment of small departures from the equilibrium configurations. Unfortunately, the corresponding equations of motion for the shells considered here would be considerably more complicated and their analysis completely out of the scope of the present research. We, nevertheless, expect that such treatment, if appropriately carried out, would also agree with the results found in [1] as the 'thin shell' limit is approached.

8. Shells with two or more values of the angular momentum

It is rather simple to extend the analysis of the previous sections to the case where the angular momentum of the particles takes on a discrete, finite set of values. Instead of (13), we have

$$\Phi(E, L^2) = \sum_i F_i(E)\ \Theta(E_i - E)\ \delta(L - L_i), \tag{61}$$

where the functions $F_i \geqslant 0$ are arbitrary, with $i = 1, 2, \ldots, N$, and N finite. We will restrict to the case of two separate values ($N = 2$), since, as will be clear from the treatment, the extension to a larger number of components is straightforward. We are actually interested in the behavior of these shells as they approach a common thin shell limit. Therefore, we will further simplify our Ansatz to the form

$$F_i(E) = Q_i E = Q_i \sqrt{B\left(1 + (p^r)^2 A + \frac{L_i^2}{r^2}\right)}, \tag{62}$$

where $Q_i \geqslant 0$ are constants. With this choice we may perform the integrals in (14) explicitly and, after some simplifications, we obtain

$$\begin{aligned}
\frac{\mathrm{d}m}{\mathrm{d}r} &= \frac{C_1\left[2\left(L_1^2 + r^2\right)B + r^2E_1^2\right]\sqrt{r^2E_1^2 - \left(L_1^2 + r^2\right)B}}{r^3B} \\
&\quad + \frac{C_2\left[2\left(L_2^2 + r^2\right)B + r^2E_2^2\right]\sqrt{r^2E_2^2 - \left(L_2^2 + r^2\right)B}}{r^3B} \\
\frac{\mathrm{d}B}{\mathrm{d}r} &= \frac{2mB}{r(r-2m)} + \frac{2C_1\left[r^2E_1^2 - \left(L_1^2 + r^2\right)B\right]^{3/2}}{r^3(r-2m)} + \frac{2C_2\left[r^2E_2^2 - \left(L_2^2 + r^2\right)B\right]^{3/2}}{r^3(r-2m)},
\end{aligned} \tag{63}$$

where $C_i = 16\pi^2 L_i Q_i/3$, $i = 1, 2$. We also find

$$\begin{aligned}
\rho(r) &= \frac{C_1\left[2\left(L_1^2 + r^2\right)B + r^2E_1^2\right]\sqrt{r^2E_1^2 - \left(L_1^2 + r^2\right)B}}{4\pi r^5B} \\
&\quad + \frac{C_2\left[2\left(L_2^2 + r^2\right)B + r^2E_2^2\right]\sqrt{r^2E_2^2 - \left(L_2^2 + r^2\right)B}}{4\pi r^5B} \\
p(r) &= \frac{C_1\left[r^2E_1^2 - \left(L_1^2 + r^2\right)B\right]^{3/2}}{4\pi Br^5} + \frac{C_2\left[r^2E_2^2 - \left(L_2^2 + r^2\right)B\right]^{3/2}}{4\pi Br^5} \\
p_T(r) &= \frac{3C_1L_1^2\sqrt{r^2E_1^2 - \left(L_1^2 + r^2\right)B}}{8\pi r^5} + \frac{3C_2L_2^2\sqrt{r^2E_2^2 - \left(L_2^2 + r^2\right)B}}{8\pi r^5}.
\end{aligned} \tag{64}$$

It is clear that we recover the results of the previous sections if we set either C_1 or C_2 equal to zero.

It will be convenient to define separate contributions to the density, ρ_1 and ρ_2, for the particles with L_1 and L_2:

$$\begin{aligned}\rho_1(r) &= \frac{C_1\left[2\left(L_1^2+r^2\right)B + r^2E_1^2\right]\sqrt{r^2E_1^2 - \left(L_1^2+r^2\right)B}}{4\pi r^5 B}\\ \rho_2(r) &= \frac{C_2\left[2\left(L_2^2+r^2\right)B + r^2E_2^2\right]\sqrt{r^2E_2^2 - \left(L_2^2+r^2\right)B}}{4\pi r^5 B}.\end{aligned} \tag{65}$$

Then, provided the integrations cover the supports of both ρ_1 and ρ_2, we have

$$M_2 - M_1 = \Delta M = \Delta m_1 + \Delta m_2, \tag{66}$$

where

$$\Delta m_1 = \int 4\pi r^2 \rho_1 \,\mathrm{d}r, \qquad \Delta m_2 = \int 4\pi r^2 \rho_2 \,\mathrm{d}r. \tag{67}$$

These expressions may be considered as the contributions to the mass from each class of particles. This will be used in the next section to compare numerical results with the thin shell limit.

Equations (63) may be numerically solved for appropriate values of the constants C_i, E_i and L_i, and initial values, i.e. for some r, of $m(r)$ and $B(r)$. We remark that, as in the previous sections, it is understood in (63), and also in (64), that both $\sqrt{r^2E_i^2 - \left(L_i^2+r^2\right)B}$ and $\left[r^2E_i^2 - \left(L_i^2+r^2\right)B\right]^{3/2}$ must be set equal to zero for $r^2E_i^2 \leqslant \left(L_i^2+r^2\right)B$. In this general case, it is clear that the shells (where by a 'shell' we mean here the set of particles having the same angular momentum L_i) may be completely separated or they may overlap only partially. We are particularly interested in the limit of a common thin shell for the chosen values of L_i. One way of ensuring that at least one of the shells completely overlaps the other is the following. We choose an inner mass M_1 and an inner radius r_i. This implies $m(r_i) = M_1$, while $B(r_i) = B_i$ is arbitrary. If we choose now arbitrary values for L_1 and L_2, the density ρ will vanish at $r = r_i$ if we choose

$$\begin{aligned}E_1^2 &= \frac{B_i\left(L_1^2+r_i^2\right)}{r_i^2}\\ E_2^2 &= \frac{B_i\left(L_2^2+r_i^2\right)}{r_i^2}.\end{aligned} \tag{68}$$

Actually we also need to impose

$$\begin{aligned}L_1^2 &> \frac{r_i^2 M_1}{r_i - 3M_1}\\ L_2^2 &> \frac{r_i^2 M_1}{r_i - 3M_1}\end{aligned} \tag{69}$$

to make sure that $r = r_i$ is the *inner* and not the *outer* boundary of the shells. We shall assume from now on that $L_2 > L_1$. Since, using the same arguments as in the single shell case, the shells have finite extension, it follows that one of the shells will be completely contained in the other.

In the next section we display some numerical results, both for thick shells that overlap partially, and for shells approaching the thin shell limit. We again find that the limit is associated with large values of C_i, and that the parameters describing the shells approach the thin shell values found in [1].

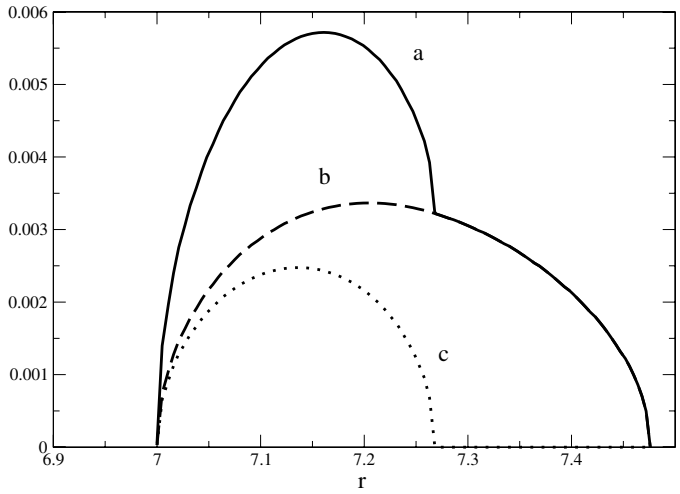

Figure 4. Plots of $\rho(r)$ (curve **a**, solid), $\rho_1(r)$ (curve **c**, dotted) and $\rho_2(r)$ (curve **b**, dashed), as functions of r for $r_i = 7.0$, $M_1 = 1.0$, $L_1 = 5$, $L_2 = 6.5$, $E_1^2 = 1.51\ldots$, $E_2^2 = 1.86\ldots$ and $C_1 = 5$, $C_2 = 3$. The end point of the plot is at $r_o = 7.4764\ldots$, with $B(r_o) = 1.0606\ldots$ and $M_2 = m(r_o) = 2.1338\ldots$.

9. Numerical results for two component systems

As a first example we take $L_1 = 5$, $L_2 = 6.5$, $r_i = 7$ and $M_1 = 1$. We also set $B(r_i) = 1$, for simplicity. Then, from (68), we set $E_1^2 = 1.510\ldots$, $E_2^2 = 1.862\ldots$. Finally, we choose $C_1 = 5$, $C_2 = 3$, and carry out the numerical integration. The results obtained indicate that the particles with $L_1 = 5$ are contained in the region $7.0 \leqslant r \leqslant 7.2682\ldots$, while for $L_2 = 6.5$ the corresponding range is $7.0 \leqslant r \leqslant 7.4764\ldots$. The resulting value of the external mass in $M_2 = 2.1338\ldots$. In figure 4 we display the total density ρ as a function of r (solid curve), as well as the contributions ρ_1 and ρ_2 to the density from the particles with respectively $L_1 = 5$ (dashed curve) and with $L_2 = 6.5$ (dotted curve).

As an illustration of the approach to the thin shell configuration we considered again the previous values $L_1 = 5$, $L_2 = 6.5$, $r_i = 7$, $M_1 = 1$, $B(r_i) = 1$, but chose $C_1 = 800$, $C_2 = 240$, and carried out the numerical integration. Figure 5 displays the functions $\rho(r)$ (solid curve), $\rho_1(r)$ (dashed curve) and $\rho_2(r)$ (dotted curve). We see that now the shell extends only to the region $r_i = 7.0 \leqslant r \leqslant r_o = 7.020\ldots$, i.e. its thickness is less than 1% of its radius. The mass, on the other hand, increases by roughly a factor of 2, since $M_2 = m(r_o) = 2.022\ldots$.

We may compare these results with those of the thin shell limit of [1] as follows. It can be seen from (29) and (31) in [1] that for a thin shell of radius R, inner mass M_1 and outer mass M_2, with two components with angular momenta L_1 and L_2, the ratio of the contributions of each component to the total mass is given by

$$\frac{\Delta m_2}{\Delta m_1} = \frac{\left(\tilde{L}_0^2 - L_1^2\right)\left(R^2 + L_2^2\right)}{\left(L_2^2 - \tilde{L}_0^2\right)\left(R^2 + L_1^2\right)}, \tag{70}$$

where $\tilde{L}_0$ is given by (40). The numerical integration gives $\Delta m_1 = 0.4545\ldots$, $\Delta m_2 = 0.5708\ldots$. If we now take $R = 7$ and solve (70) for $\tilde{L}_0$ we find $\tilde{L}_0 = 5.8079\ldots$, while replacement in (40) gives $\tilde{L}_0 = 5.8386\ldots$, which we consider as a good agreement, with a discrepancy of the order of the ratio of thickness to radius.

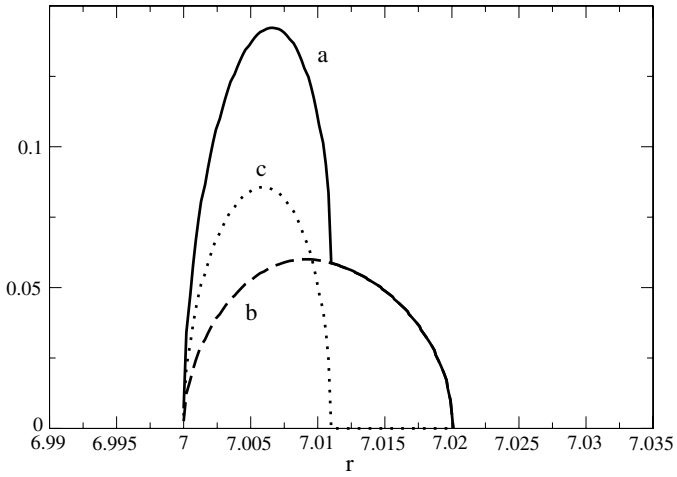

Figure 5. Plots of $\rho(r)$ (curve **a**, solid), $\rho_1(r)$ (curve **c**, dotted) and $\rho_2(r)$ (curve **b**, dashed), as functions of r for $r_i = 7.0$, $M_1 = 1.0$, $L_1 = 5$, $L_2 = 6.5$, $E_1^2 = 1.51\ldots$, $E_2^2 = 1.86\ldots$ and $C_1 = 800$, $C_2 = 240$. The end point of the plot is at $r_o = 7.020\ldots$, with $B(r_o) = 1.0026\ldots$ and $M_2 = m(r_o) = 2.022\ldots$.

10. Final comments and conclusions

The general conclusion from this work is that one can effectively construct a wide variety of models satisfying the restriction that L takes only a finite set of values, and that they do seem to contain the models used in [1] as appropriate thin shell limits. We also remark that the starting point for our construction is a variant of the Ansatz used in [7], where f is factored in E- (the particle energy) and L-dependent terms. The possibility of multi-peaked structure in the case of more than one value of L obtained here is also in correspondence with the general results obtained in [7].

Acknowledgments

This work was supported in part by grants from CONICET (Argentina) and Universidad Nacional de Córdoba. RJG and MAR are supported by CONICET. We are also grateful to H Andreasson for his helpful comments, and to the anonymous referees for their constructive comments and criticisms.

References

[1] Gleiser R J and Ramirez M A 2009 *Class. Quantum Grav.* **26** 045006
[2] Evans A B 1977 *Gen. Rel. Grav.* **8** 155
[3] Einstein A 1939 *Ann. Math.* **40** 922
[4] Rein G 1994 *Math. Proc. Camb. Phil. Soc.* **115** 559–70
[5] Rein G and Rendall A 2000 *Math. Proc. Camb. Phil. Soc.* **128** 363–80
[6] Andreasson H 2005 The Einstein–Vlasov system/kinetic theory *Living Rev. Relativ.* **8** 2 http://www.livingreviews.org/lrr-2005-2, and references therein.
[7] Andreasson H and Rein G 2007 *Class. Quantum Grav.* **24** 1809
[8] Andreasson H 2007 *Commun. Math. Phys.* **274** 409–25
[9] Andreasson H 2008 *J. Differ. Equ.* **245** 2243–66
[10] Andreasson H and Rein G 2006 *Class. Quantum Grav.* **23** 3659